...UMENTATION PAGE

Form Approved
OMB No 0704-0188

1a REPORT SECURITY CLASSIFICATION Unclassified	1b RESTRICTIVE MARKINGS
2a SECURITY CLASSIFICATION AU...ORITY	3 DISTRIBUTION/AVAILABILITY OF REPORT DISTRIBUTION STATEMENT A Approved for public release Distribution Unlimited
2b DECLASSIFICATION / DOWNG...DING SCHEDULE	
4 PERFORMING ORGANIZATION REPORT NUMBE...S)	5 MONITORING ORGANIZATION REPORT NUMBER(S)
6a NAME OF PERFORMING ORGANIZATION Dept. of Chemistry Cornell University	6b OFFICE SYMBOL (If applicable)
6c ADDRESS (City, State, and ZIP Code) Dept. of Chemistry Cornell University Ithaca, NY 14853	7a NAME OF MONITORING ORGANIZATION Office of Naval Research 7b ADDRESS (City, State, and ZIP Code) Chemistry Program 800 N. Quincy Street Alexandria, VA 22217
8a NAME OF FUNDING / SPONSORING ORGANIZATION Office of Naval Research	8b OFFICE SYMBOL (If applicable)
8c ADDRESS (City, State, and ZIP Code) Chemistry Program 800 N. Quincy St. Alexandria, VA 22217	9 PROCUREMENT INSTRUMENT IDENTIFICATION NUMBER N00014-91-J-1269 10 SOURCE OF FUNDING NUMBERS

PROGRAM ELEMENT NO	PROJECT NO	TASK NO	WORK UNIT ACCESSION NO

11 TITLE (Include Security Classification)

Unclassified: Synthesis, Structure, and Properties of Anti-perovskite Nitrides Ca_3MN, M=P, As, Sb, Bi, Ge, Sn, and Pb

12 PERSONAL AUTHOR(S)

Ming Y. Chern, D.A. Vennos, and F.J. DiSalvo

13a TYPE OF REPORT	13b TIME COVERED	14 DATE OF REPORT (Year, Month, Day)	15 PAGE COUNT
Technical Rpt. #8	FROM 1990 TO 1993	May 30, 1991	

16 SUPPLEMENTARY NOTATION

17 COSATI CODES			18 SUBJECT TERMS (Continue on reverse if necessary and identify by block number)
FIELD	GROUP	SUB-GROUP	Solid State Compounds; Electrical Properties; Nitrides; Magnetic Properties; Anti-Perovskites

19 ABSTRACT (Continue on reverse if necessary and identify by block number)

A family of anti-perovskite nitrides of the formula Ca_3MN, where M is a Group IV or a Group V element, is reported. Ca_3BiN, synthesized by mixing and pressing powders of Ca_3N_2 and Bi into a pellet and subsequently heating the pellet at 1000°C in flowing, dry N_2 gas, is prototypical of this family of compounds. The bismuth in Ca_3BiN has an uncommon oxidation state of 3- as suggested by the properties (semiconducting and diamagnetic) of the compound. The anionic bismuth can be subsitituted for by other trivalent anions Sb^{3-}, As^{3-}, and P^{3-} as expected. The structure of Ca_3AsN and Ca_3PN are distorted from the simple cubic anti-perovskite cell at room temperature because of the small size of As^{3-} and P^{3-}. More interestingly, Ca_3N_2 also reacts with Ge, Sn, and Pb at 1300°C to form similar anti-perovskites, resulting in metallic phases and the unusual open shell oxidation state of 3- for the Group IV elements.

20 DISTRIBUTION / AVAILABILITY OF ABSTRACT	21 ABSTRACT SECURITY CLASSIFICATION
☒ UNCLASSIFIED/UNLIMITED ☒ SAME AS RPT ☐ DTIC USERS	Unclassified
22a NAME OF RESPONSIBLE INDIVIDUAL Dr. Mark Ross	22b TELEPHONE (Include Area Code) 202-696-4409 22c OFFICE SYMBOL

Synthesis, Structure, and Properties of Anti-perovskite Nitrides Ca_3MN, M= P, As, Sb, Bi, Ge, Sn, and Pb

Ming Y. Chern, D. A. Vennos, and F. J. DiSalvo*

Department of Chemistry

Cornell University

Ithaca, New York 14853

Abstract

A family of anti-perovskite nitrides of the formula Ca_3MN, where M is a Group IV or a Group V element, is reported. Ca_3BiN, synthesized by mixing and pressing powders of Ca_3N_2 and Bi into a pellet and subsequently heating the pellet at 1000°C in flowing, dry N_2 gas, is prototypical of this family of compounds. The bismuth in Ca_3BiN has an uncommon oxidation state of 3- as suggested by the properties (semiconducting and diamagnetic) of the compound. The anionic bismuth can be substituted for by other tri-valent anions Sb^{3-}, As^{3-}, and P^{3-} as expected. The structure of Ca_3AsN and Ca_3PN are distorted from the simple cubic anti-perovskite cell at room temperature because of the small size of As^{3-} and P^{3-}. More interestingly, Ca_3N_2 also reacts with Ge, Sn, and Pb at 1300°C to form similar anti-perovskites, resulting in metallic phases and the unusual open shell oxidation state of 3- for the Group IV elements.

Introduction

The perovskite structure with the formula ABX_3 is adopted by many oxide compounds, where A and B are cations and X is oxygen. The structure, which emphasizes the twelve fold coordination of the A atom, can be described by a cubic unit cell which contains an A atom at the center of a cube, B atoms at the corners and X atoms at the center of the cell edges. Another common way to describe the structure is to shift the origin so that a B atom is at the center of the cube, A atoms at the corners and X atoms on the face centers. The latter emphasizes the octahedral coordination of the B atom by six X atoms. Anti-perovskite structures, in which X and B interchange their roles, are also known (*1*); i. e. the X anion is at the cationic B site instead and becomes the center of an octahedron formed by six metal atoms.

Among nitride anti-perovskites two classes can be further distinguished. In the first class, nitrogen can be thought of as an interstitial atom which goes into the octahedral hole of an already existing metal framework with a slightly modified cell constant. Therefore, extensive metal-metal bonding continues to exist in the nitride. Examples of this class are Mn_4N (3.857Å), Fe_4N (3.795Å), and Fe_3PtN (3.857Å), whose original compounds are fcc manganese (3.862Å), fcc iron (3.666Å) and Fe_3Pt (Cu_3Au structure) (3.727Å), respectively (*2*). The cell constant is listed in the parenthesis following each compound for comparison. Note that the inclusion of interstitial nitrogen causes only a small change in lattice parameter.

The new anti-perovskite nitrides reported in this paper, i. e. Ca_3MN, where M is a Group IV or Group V element, belong to the second class. In this class, the A and B sites are occupied by anions M^{3-} and N^{3-} respectively, and the X sites are occupied by cations Ca^{2+}, thus the cation and anion positions are completely reversed from a normal oxide perovskite. Note that the Ca_3M intermetallics do not exist for the Group IV or V element, except for Ca_3Pb (3), in contrast to the first class of interstitial nitrides.

Oxide perovskites, though simple in structure, exhibit many interesting properties such as structural phase transitions, ferroelectricity, and superconductivity (4), etc.. Furthermore there are many oxide compounds which are often considered as derivatives of the perovskite structure such as the K_2NiF_4 structure. The compounds in this new family of nitrides also exhibit interesting physical phenomena. The synthesis, characterization, and properties of these new phases are described in the following sections.

Sample preparation

Since some of the reactants and products are air-sensitive, all sample manipulations were carried out in an Ar filled glove box. Calcium nitride (Ca_3N_2) was first prepared by heating granular calcium (~0.3X0.3X0.3cm^3) in an N_2 atmosphere at 900°C. The product was then ground into a fine powder and mixed with the third element (in powdered form) stoichiometrically. Pressed pellets of the mixtures were heated in N_2 at 1000°C for two days to make the P, As, Sb, Bi compounds. Special care was

taken to synthesize the phosphorus compound by sealing the pellet in a quartz tube and pre-heating the pellet at 200°C for five hours to avoid producing white phosphorus.

For Ge, Sn and Pb, however, a higher temperature, 1300°C, was necessary to make the cubic phase. To prevent losing materials at such a high temperature, the samples were sealed in niobium tubes (3/8". diameter, 0.022" thick wall, 3" long) by arc welding in an Ar atmosphere before the reaction. Since one nitrogen atom is released from every Ca_3N_2 unit when the compound is formed, the amount of sample that can be sealed in the tube is limited to approximately 0.001mole so that the maximum nitrogen pressure, ~20atm, did not blow up the tube. Non-cubic germanium and tin phases were formed when the reaction temperature was reduced to 1000°C. Though a cubic Ca_3PbN was found at 1000°C, the lattice constant is smaller than that of the one made at high temperatures and the x-ray diffraction peaks are rather broad, indicating some kind of disorder. Attempts to make the anti-perovskite analogues with carbon and silicon have not yet been successful.

The colors of the samples are yellow, red, gray, and black for the phosphorus, arsenic, antimony, and bismuth compounds respectively. All the germanium, tin, and lead compounds have a dark metallic luster and become black powders after grinding. All samples are air sensitive and readily decompose in moist air to release NH_3.

Structure Determination

X-ray powder diffraction data were collected on a Scintag XDS 2000 automated diffractometer using Cu $K\alpha$ radiation. The $K\alpha_2$ lines were stripped using Scintag software. The powder samples were covered with a thin layer of Mylar, 0.5 mil. in thickness, to avoid air exposure when the data were taken. The patterns from the cubic phases of Ge, Sn, Pb, Sb, and Bi were indexed and solved by trial and error. The lattice parameters were refined by a least-square fit and are shown in **Table I**. Theoretical intensities based on the cubic anti-perovskite structure were calculated and matched well with the experimental integrated intensities. **(Table II & Table III)**. No superlattice lines or splitting of peaks due to possible distortions from the perfect cubic cell were detected within the limit of the machine (intensity limit: 0.3% of the strongest peak; typical peak width: 0.09° FWHM at 30° in 2θ).

The arsenic and phosphorus compounds, however, show clear splitting of the cubic diffraction lines and extra "superlattice" peaks (see **Fig. 1 & Fig. 2**). The true symmetry for Ca_3AsN at room temperature is orthorhombic, which was not known until the distorted structure was completely solved because the "a" and "b" (**Table I**) are so close that we could not resolve them in our diffractometer. (The Miller indices used in **Fig. 1** are therefore based on a pseudo-tetragonal cell.) The distorted structure of Ca_3AsN involves tilts of the nitrogen-centered octahedra along three axes. It has been solved by Rietveld refinement of neutron and x-ray powder diffraction data, and will be reported separately (5).

Magnetic Susceptibility Measurement

The magnetic susceptibility of the Bi, Sb, As, and P compounds was measured between 320 K and 4 K by the use of a Faraday balance (*6*). The susceptibility at room temperature was measured at different fields to subtract small ferromagnetic impurity signals from the data using the method of Owen and Honda (*7*). The extent of such ferromagnetic contaminations is very small, on the order of 10^{-6}g Fe, and is likely picked up as small particles when handling the sample in the glove box. Except for a small amount of paramagnetic impurities showing Curie-like behavior at low temperatures (<150K), the susceptibilities of the samples are diamagnetic and temperature independent below 320K. The intrinsic susceptibility of the samples was obtained by subtracting the Curie susceptibility and is tabulated in **Table IV**. The theoretical value (*8*) is also presented in the table for comparison by assuming a simple ionic picture and the "additive rule".

The experimental values are smaller than the calculated ones due to two reasons: First, the ionic picture is not totally correct and covalency between the species produces positive susceptibility, i. e. Van Vleck paramagnetism. Alternatively, the covalency decreases the effective radius of the anions, especially rapidly for N^{3-}, and thus also reduces the core diamagnetism, since it is proportional to the square of the ion radius. Second, the phosphorous and arsenic compounds are distorted at room temperature, resulting in a stronger bonding between the P or As anion and the Ca cation, hence the susceptibility increases due again to the Van Vleck paramagntism.

The susceptibility of the As compound was measured at high temperatures, up to 1200K, by using a furnace to heat the sample at 100K/hr (**Fig. 3**). It is likely that the decreasing susceptibility with increasing temperature indicates that the magnitude of the distortion is decreasing and when the susceptibility is no longer temperature dependent the compound is cubic. Diffraction data reported elsewhere shows that the distortion does in fact increase when the temperature is decreased from 300K to 10K (*5*). From the data of **Fig. 3** the transition to cubic symmetry would occur near 1025K. The high temperature susceptibility is closer to the calculated value (see **Table IV**) presumably due to a decrease of the Van Vleck term. A similar transition occurs in the phosphorus compound at a slightly higher temperature, 1070 K (**Fig. 4 & Table IV**).

Electrical Conductivity Measurements

Four-probe conductivity measurements were performed at 13 Hz by lock in detection on pellets of Ca_3BiN and Ca_3PbN sintered at 1000°C. The sample dimensions were 1/2" in diameter and 0.050" in thickness. Four spring-loaded pins arranged in a colinear configuration were pressed against the pellet to serve as the contacts, which were shown to be ohmic from the linearity of the I-V characteristic up to the maximal current applied, ~70 mA. To prevent air exposure, the moisture-sensitive sample was mounted on a supporting stage and covered in the glove box by a Lucite cap which also supports the four spring-loaded pins.

We calibrated the system by measuring the resistance of a solid

molybdenum sample of the same thickness and diameter as the nitride samples, and a proportionality constant between the resistivity and the resistance of the Mo was obtained (9). This value was then used to convert the resistance to the resistivity for the sample. This conversion is valid if we measure the isotropic conductivity of a randomly oriented polycrystalline sample or a material of cubic symmetry.

The temperature dependence of the resistivity of Ca_3BiN from 4K to 320K is shown in **Fig. 5**. The magnitude of the resistivity indicates that Ca_3BiN is a semiconductor. However, the small positive temperature dependence suggests that there are conducting states due to overlap of the wave functions of the electrons, or holes induced by the impurities or defects in the sample; that is, this material is an "impurity band" conductor. The turn-around at 20K probably comes from the "freeze-out" of some of those charge carriers.

The resistivity of Ca_3PbN is much smaller than that of Ca_3BiN, as expected. The room temperature value of $5x10^{-4}\Omega\cdot cm$ is large for a non-transition metal compound and is near the minimum metallic conductivity expected for one carrier per unit cell. The small resistance ratio ($\rho(4.2K) = 1.7x10^{-4}\Omega\cdot cm$) indicates that the sample has a high impurity/defect level or perhaps that the intergrain resistivity of the polycrystalline pellet is large.

The resistance of a small pellet of Ca_3SbN at room temperatures was measured by an ohmmeter; the value, 10 kohm, indicates that it is a semiconductor. The ohmmeter registered "infinity" for the insulating As and P compounds. At room temperature the two point resistance of the Pb, Sn, and Ge nitride samples was lower than the ohmmeter resolution of

0.01ohms.

Discussion

The formal oxidation state of the Group V atoms M in Ca_3MN is 3-. This anionic behavior of the Group V elements is seldom seen in oxides, but is common in intermetallic compounds of M with electropositive elements. For example, M also has 3- oxidation state in M'_3M (*10*), where M' is an alkali metal and M is P, As, Sb, or Bi. The assignment of the 3- oxidation state implies the following scheme for the band structure: The calcium 4s band is empty, but the bismuth 6p bands and nitrogen 2p bands should be full. So the solid has a filled valence band derived mainly from the Bi-6p orbital and empty conduction bands above the Fermi level derived mainly from the Ca orbitals. The calculated band structure shows that Ca_3BiN has a small band gap of 0.2 eV (*11*). This is consistent with the observation that Ca_3BiN is quite susceptible to impurities to form impurity "bands".

When the bismuth is substituted for by other trivalent anions, Sb^{3-}, As^{3-}, and P^{3-}, the band gap is expected to increase in sequence, because the electronegativity of the anions increases, corresponding to a decrease of the energy of the p levels of the anions relative to the calcium levels. The color of the compounds (black, gray, red, and yellow for the Bi, Sb, As, P, respectively) supports the above picture. More interestingly, Bi, Sb, and As can also be replaced by their left neighboring elements in the periodic table, namely, Pb, Sn, and Ge. Therefore, these Group IV metals also have an

oxidation state of 3-, again an unknown state in oxide chemistry. These new phases should be metallic because the Group IV element has one electron less than the Group V neighbors so that their p shell is not completely filled, resulting in a partially filled valence band if we apply the same band structure scheme mentioned above, i.e., we assume a rigid band approximation. The calculated band structure also shows that the Fermi level of Ca_3PbN lies below the top of the valence band (*11*). A search for the "electron-doped" analogue of the anti-perovskite by substituting Bi with Group VI elements such as Te has not yet been successful. However, we have been able to make a pseudo-quaternary compound $Ca_3Bi_{1-x}Pb_xN$ (x = 0.5) with a lattice constant intermediate between those of the Bi and the Pb phases (a=4.925Å).

Since the radii of As^{3-} and P^{3-} are smaller than that of Bi^{3-}, we should expect that cubic Ca_3AsN and Ca_3PN are not structurally stable from the geometrical argument that As^{3-} and P^{3-} are too small to completely fill the hole formed by their twelve calcium neighbors in O_h symmetry. The room temperature structure of these two members are in fact distorted from cubic as expected. Although we did not perform a high temperature x-ray study, the phase transitions detected at 1025K and 1070K in the high temperature magnetic susceptibility for the arsenic and the phosphorus phases are likely the structural phase transitions corresponding to the change of the crystal structure from the distorted phase to the cubic anti-perovskite. At high temperatures, the effective radii of As^{3-} and P^{3-} are larger due to thermal vibrations, hence the cubic structure is expected to be the stable one. The phosphorus compound undergoes a similar transition

at a higher temperature as may also be expected from the smaller ionic radius of P^{3-}. Such transitions to the cubic phase at high temperatures in distorted oxide perovskites are rather common (*4*).

The diamagnetic susceptibility of the Bi, Sb, As, and P compounds, respectively, decreases from Bi to P because the radius of the trivalent anion decreases from Bi to P and the Larmor diamagnetism is proportional $\langle r \rangle^2$, where $\langle r \rangle$ is the mean radius of the ionic species. One can roughly estimate the radius of Bi^{3-} from the accepted ionic radius of Ca^{2+} (1.0Å (*12*)) and the lattice constant by assuming that the spherical Bi^{3-} just touches its twelve calcium neighbors. The value thus obtained is 2.4 Å, which is much larger than either that of atomic Bi, 1..5Å, or that of Bi^{3+} (1.0Å (*12*)), but is compatible with those of Bi^{3-} anions in the intermetallics of bismuth and alkali metals, i. e. 2.2Å, 2.2Å, 2.3Å, and 2.3Å for the hexagonal $BiLi_3$, $BiNa_3$, BiK_3, and $BiRb_3$, respectively, (again assuming known ionic radii, 0.76Å, 1.02Å, 1.38Å, and 1.52Å for Li^+, Na^+, K^+, and Rb^+, respectively (*12*)), indicating that the Bi in this nitride compound is rather ionic and hence produces a large diamagnetism.

The average Ca-N bond distance, 2.45Å, of these anti-perovskites is close to those in Ca_3N_2 (*13*), 2.47Å, CaNiN (*14*), 2.51Å, and Ca_2ZnN_2 (*15*), 2.48Å. In the anti-perovskite compounds discussed in this paper, the nitrogen is in an octahedral hole formed by six calcium atoms. A distorted octahedral coordination of nitrogen by six metal atoms is frequently observed in the known ternary nitrides containing calcium. Examples are CaNiN (*14*), where the N is coordinated to two Ni and four Ca atoms; Ca_2ZnN_2, where the N is surrounded by five Ca atoms and one zinc atom (*15*); CaGaN, where the N has six nearest neighbors, one Ga and five Ca,

(*16*), and Ca_4In_2N, where the N is in an octahedral coordination by six calcium atoms (*17*). Even in Ca_3N_2 itself the N is coordinated by six calcium atoms in a distorted octahedron (*13*). This empirical observation is useful in building structural models to solve the structure of other ternary calcium nitrides. The only exception to the rule is the previously known Zintl phase $CaGeN_2$, where $(GeN_2)^{2-}$ adopts a β-cristobalite structure, with the calcium ions "stuffed" into tetrahedral sites; each N is coordinated by two Ge with a very short Ge-N distance of 1.85 Å and by one Ca (*18-20*).

In summary, we have investigated a series of anti-perovskite nitrides that form with Ca, N and a Group IV or V element. By varying the central anions, the properties change from metallic (Ca_3PbN, Ca_3SnN, Ca_3GeN) to semiconducting with small band gaps (Ca_3BiN, Ca_3SbN), to insulating with structural phase transitions in Ca_3AsN and Ca_3PN. Ca_3AsN appears to be the first example of a distorted anti-perovskite whose structure is known since there are few anti-perovskites in literature, and this work is reported in a separate paper (*5*).

Acknowledgements

We thank M. Hornbostel for the assistance with the Faraday measurements. We thank Prof. M. Whangbo and W. E. Pickett for the useful discussions about the band structure. We are grateful for support of this work by the Office of Naval Research.

References

1. H. Haschke, H. Nowotny and F. Benesovsky, *Monatshefte Fuer Chemie* **98,** 2157 (1967).
2. G. W. Wiener and J. A. Berger, *J. of Metals* **7,** 360 (1955).
3. V. O. Helleis, H. Kandler, E. Leicht, W. Quiring, and E. Wölfel, Z. *Anorg. Allg. Chem.* **320,** 86 (1963).
4. F. S. Galasso, "Structure, Properties and Preparation of Perovskite-Type Compounds", Pergamon, Elmsford, NY (1969).
5. M. Y. Chern, F. J. DiSalvo and J. B. Parise, to be published.
6. J. K. Vassilu, M. Hornbostel, R. Ziebarth, and F. J. DiSalvo, *J. Solid State Chem.* **81,** 208 (1989).
7. P. W. Selwood, "Magnetochemistry", p. 186, Wiley-Interscience, New York (1979).
8. J. H. Van Vleck, "The Theory of Electric and Magnetic Susceptibilities", p. 225, Oxford Univ. Press, London/New York (1952).
9. J. D. Wasscher, *Philips Res. Rep.* **16,** 301 (1961).
10. "Pearson's Handbook of Crystallographic Data for Intermetallic Phases" (P. Villars and L. D. Calvert, Eds.), Amer. Soc. Metals, Metals Park, OH (1985).
11. W. E. Pickett, private communication.
12. R. D. Shannon, *Acta Crystallogr.* **A32,** 751 (1976).
13. Y. Laurent, J. Lang, and M. T. LeBihan, *Acta Crystallogr.* **B24,** 494 (1968).

14. M. Y. Chern and F. J. DiSalvo, *J. Solid State Chem.* **88,** 459 (1990).

15. M. Y. Chern and F. J. DiSalvo, *J. Solid State Chem.* **88,** 528 (1990).

16. P. Verdier, P. L'Haridon, and R. Marchand, *Acta Crystallogr.* **B30,** 226 (1974).

17. G. Cordeied and S. Rönniger, Z. *Naturforsch* **B42,** 825 (1987).

18. M. Maunaye, J. Guyader, Y. Laurent, and J. Lang, *Bull. Soc. Fr. Minéral Cristallogr.* **94,** 347 (1971).

19. E. Zintl and G. Brauer, Z. *Physi. Chem.* **B20,** 245 (1933).

20. E. Zintl, *Angew. Chem.* **1,** 1 (1937).

Figure captions

Figure 1. X-ray powder diffraction pattern of Ca_3AsN. The pattern is indexed on a tetragonal cell, but the true symmetry is orthorhombic with "a" and "b" almost the same (see **Table 1**). Asterisk signs, *, are used to indicate impurities or second phases. The air-sensitive sample was covered by a thin layer of mylar for protection, but the mylar formed a semi-circular arc over the sample so that there were no diffraction peaks from the mylar.

Figure 2. X-ray powder diffraction pattern of Ca_3PN. The pattern is indexed on an orthorhombic cell; the broad peak at 25 degrees is from a flat mylar covering over the air-sensitive sample. Impurities or second phases are indicated by *.

Figure 3 Magnetic susceptibility of Ca_3AsN at high temperatures. Two curves are shown: one was taken on heating (o), the other one is a cooling curve (+), both were taken at a rate of 100K/hr. A phase transition at 1025K with a small hysteresis is implied for Ca_3AsN.

Figure 4. High temperature magnetic susceptibility of Ca_3PN. A phase transition at 1070K is also implied for Ca_3PN.

Figure 5. Temperature dependence of the electrical resistivity of a polycrystalline sample of Ca_3BiN.

TABLE I

THE LATTICE CONSTANTS OF THE Ca_3MN SERIES

M=Bi, Sb, As, P:		M=Pb, Sn, Ge:	
Ca_3BiN	4.8884(5)Å	Ca_3PbN	4.9550(7)Å
Ca_3SbN	4.8541(4)Å	Ca_3SnN	4.9460(6)Å
Ca_3AsN	4.77Å[a]	Ca_3GeN	4.7573(5)Å
Ca_3PN	4.73Å[b]		

[a] Distorted, orthorhombic cell: a=6.7249Å, b=6.7196Å, c=9.5336 Å; pseudo-cubic cell: a'=4.77Å ~ a/ $\sqrt{2}$ ~ b/ $\sqrt{2}$ ~ c/ 2.

[b] Distorted, orthorhombic cell: a=6.7091Å, b=9.4518Å, c=6.6581Å; pseudo-cubic cell: a'=4.73Å ~ a/ $\sqrt{2}$ ~ b/ 2 ~ c/ $\sqrt{2}$.

TABLE II

OBSERVED AND CALCULATED INTENSITIES OF Ca_3MN, M = Ge, Sn, Pb

	Ge		Sn		Pb	
hkl	$I/I_{0,obs}$	$I/I_{0,calc}$	$I/I_{0,obs}$	$I/I_{0,calc}$	$I/I_{0,obs}$	$I/I_{0,calc}$
100	<1	1	19	18	51	50
110	14	13	40	37	73	69
111	100	100	100	100	100	100
200	67	65	61	62	62	60
210	1	1	14	11	30	29
211	4	5	20	16	35	32
220	44	42	45	42	40	42
300	2	<1 *	7	1	18	3
221		1		5		13
310	2	2	8	7	18	15
311	38	39	44	41	44	43
222	17	14	12	14	15	14
320	<1	<1	5	3	7	8
321	3	3	8	8	16	17
400	7	6	7	6	6	7
410	<1	<1	5	2	11	5
322		<1		2		5
330	1	<1	4	1	8	3
411		1		3		6
331	16	16	16	17	17	19
420	18	19	19	19	17	20
421	-	-	3	2	9	8
332	-	-	-	-	5	5

* Brackets indicate that the peaks overlap.

TABLE III

OBSERVED AND CALCULATED INTENSITIES OF Ca_3MN, M = Sb, Bi

	Sb		Bi	
hkl	$I/I_{o,obs}$	$I/I_{o,calc}$	$I/I_{o,obs}$	$I/I_{o,calc}$
100	16	19	54	51
110	42	38	76	70
111	100	100	100	100
200	64	62	59	60
210	12	11	31	30
211	17	16	33	32
220	41	42	39	41
300	6	1 *	17	3
221		5		13
310	8	7	14	15
311	38	41	40	43
222	13	14	13	14
322	3	3	8	8
321	8	8	16	18
400	6	6	6	7
410	4	2	10	5
322		2		5
330	4	1	8	3
411		3		6
331	12	17	15	19
420	15	19	16	20
421	3	3	7	8

* Brackets indicate that the peaks overlap.

TABLE IV

THE MAGNETIC SUSCEPTIBILITIES OF THE Ca_3MN, M = Bi, Sb, As, AND P

Compound	$\chi_{M,\ exp}(10^{-6}emu/mole)$	$\chi_{M,\ calc}(10^{-6}emu/mole)$
Ca_3BiN	-153.5	-
Ca_3SbN	-120.4	-191.9
Ca_3AsN (300K)	-82.3	
Ca_3AsN (1150K)	-112.5	-156.9
Ca_3PN (300K)	-74.6	
Ca_3PN (1150K)	-99.0	-126.9

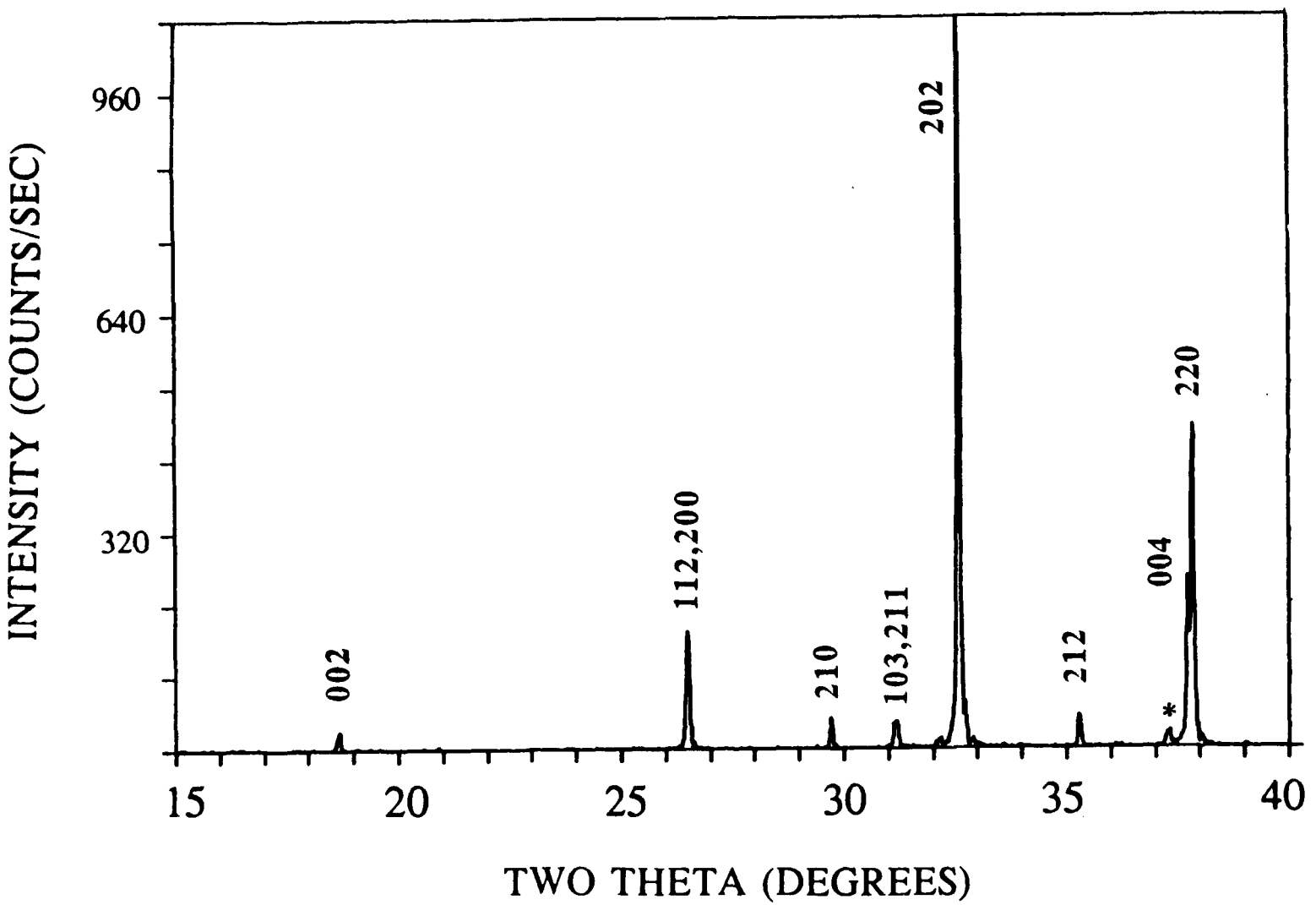

Fig. 1 (a)

Ca_3MN: Chem etal

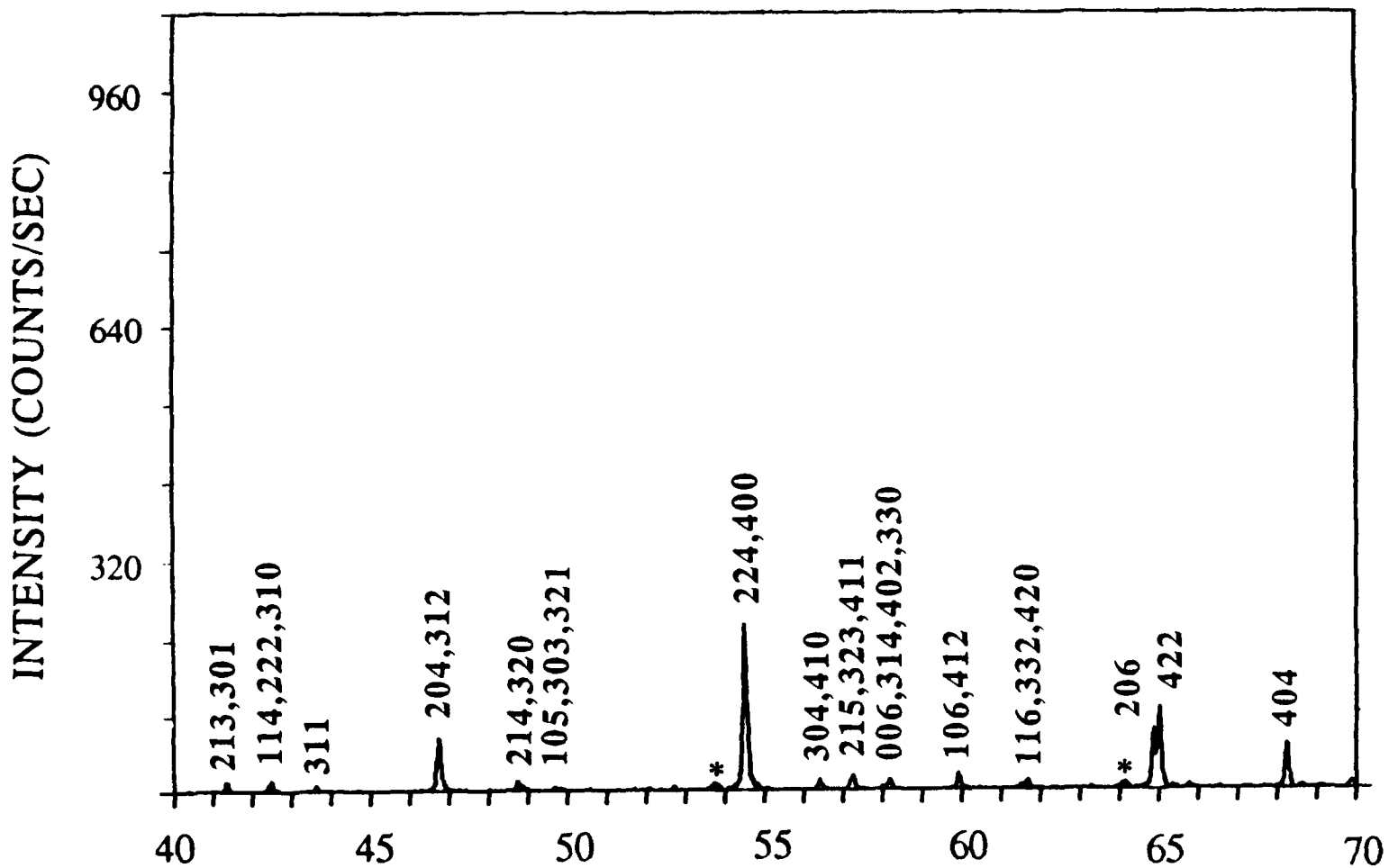

Fig 1(b)

Ca-MN : Chern et al

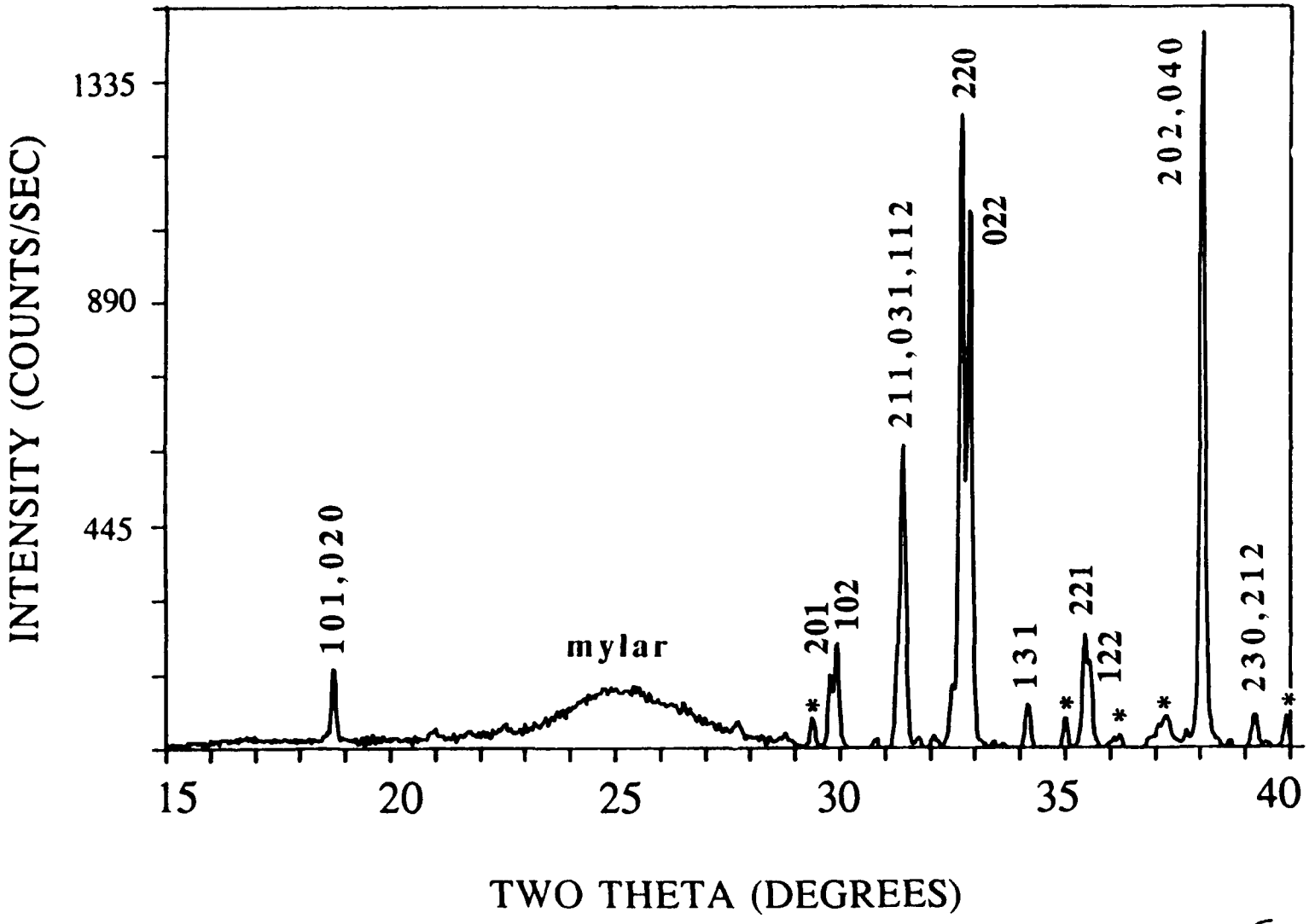

Fig 2(a)

Ca$_3$MN: Chern et al

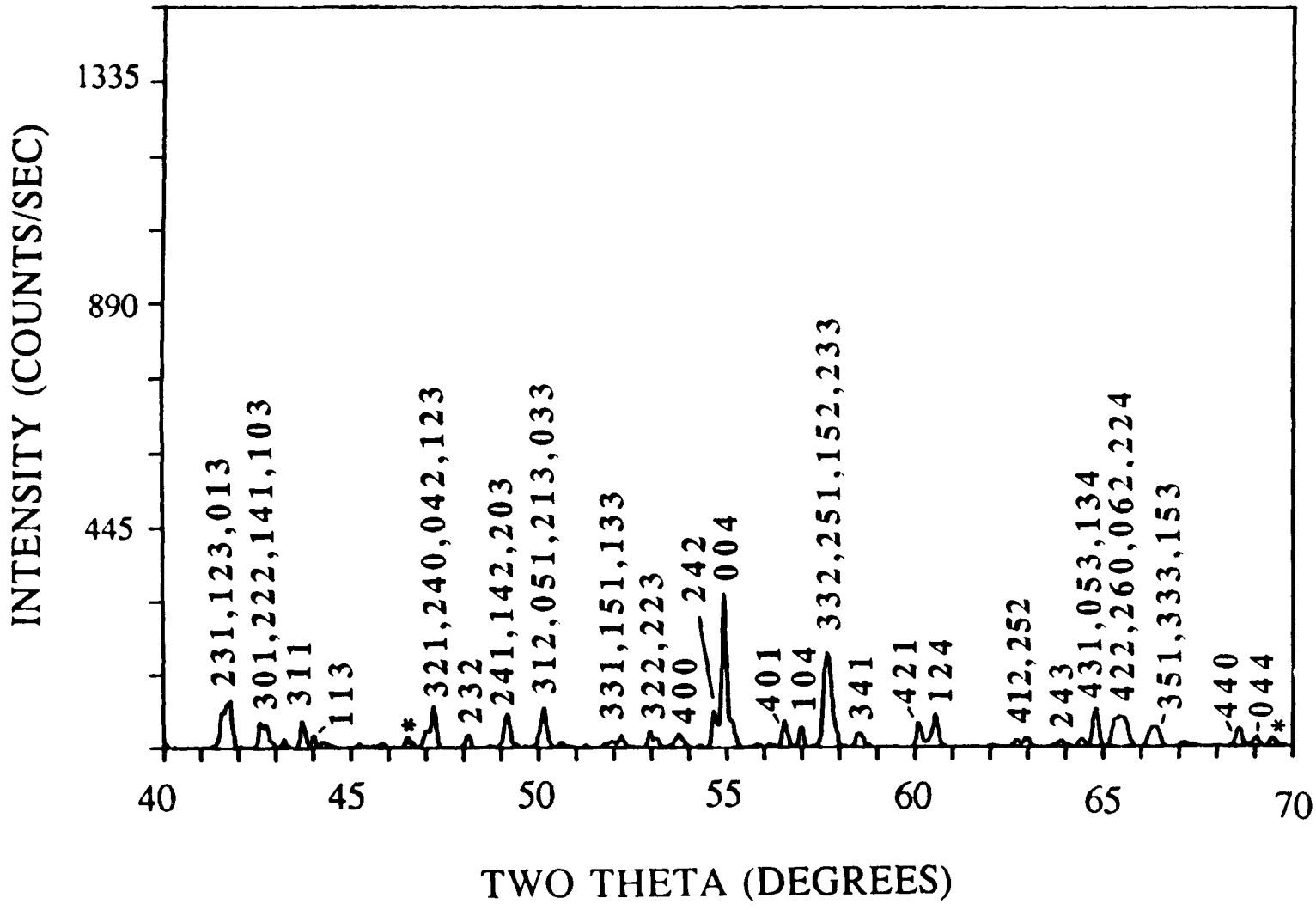

Fig 2(b)

Ca_3MN: Chem etal

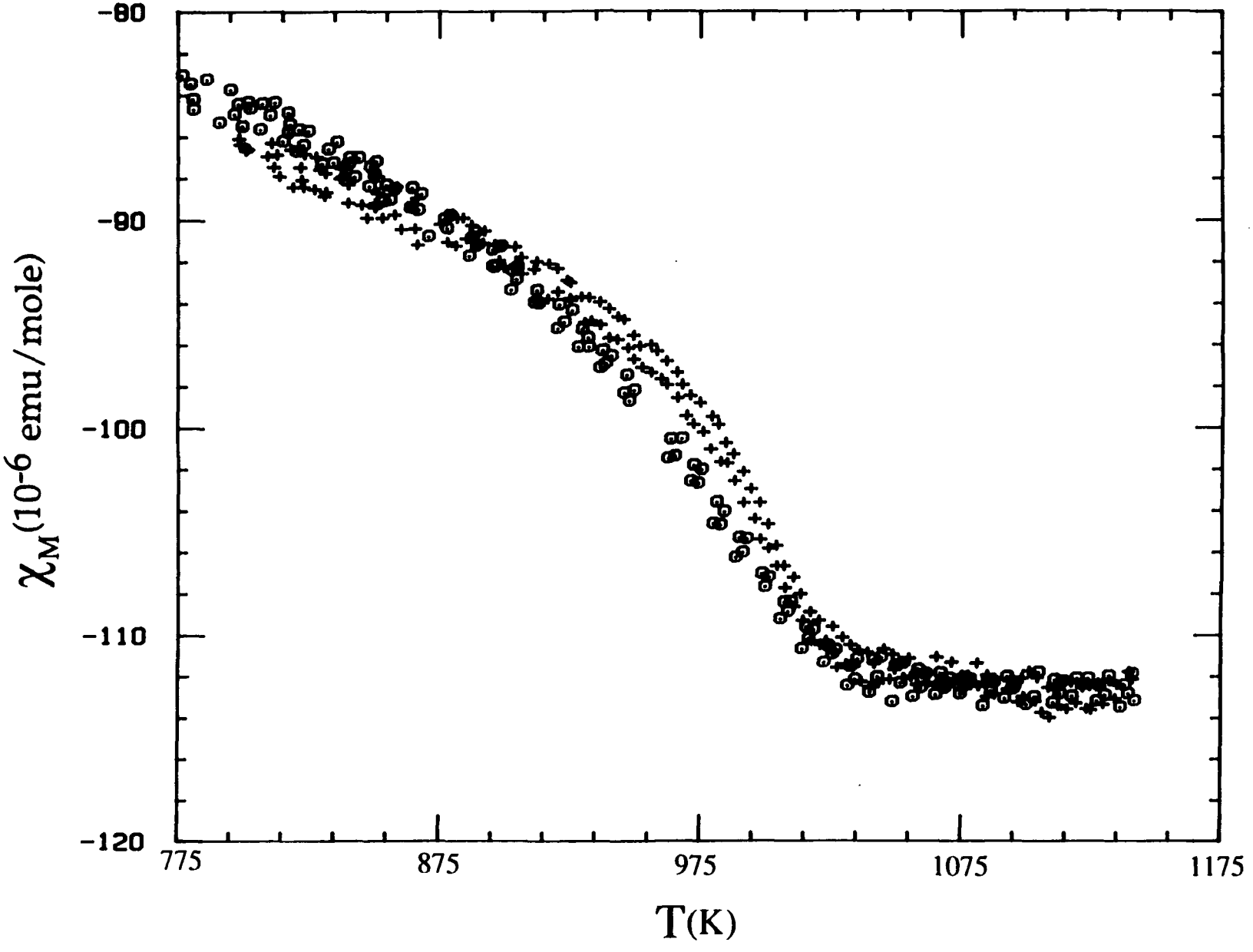

Cu_3MN Chern et al Fig 3

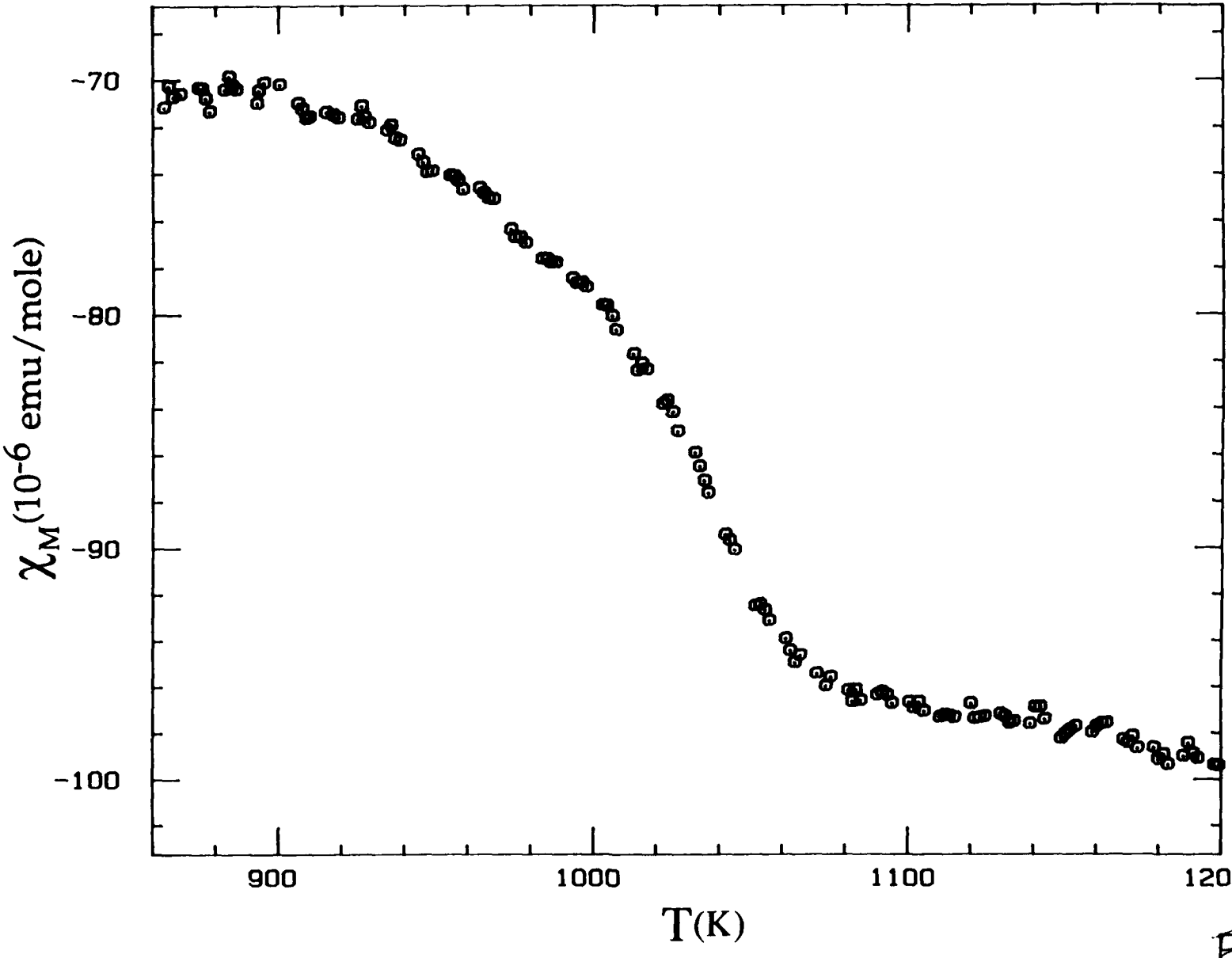

Fig 4

Ca, MN: Chem etal

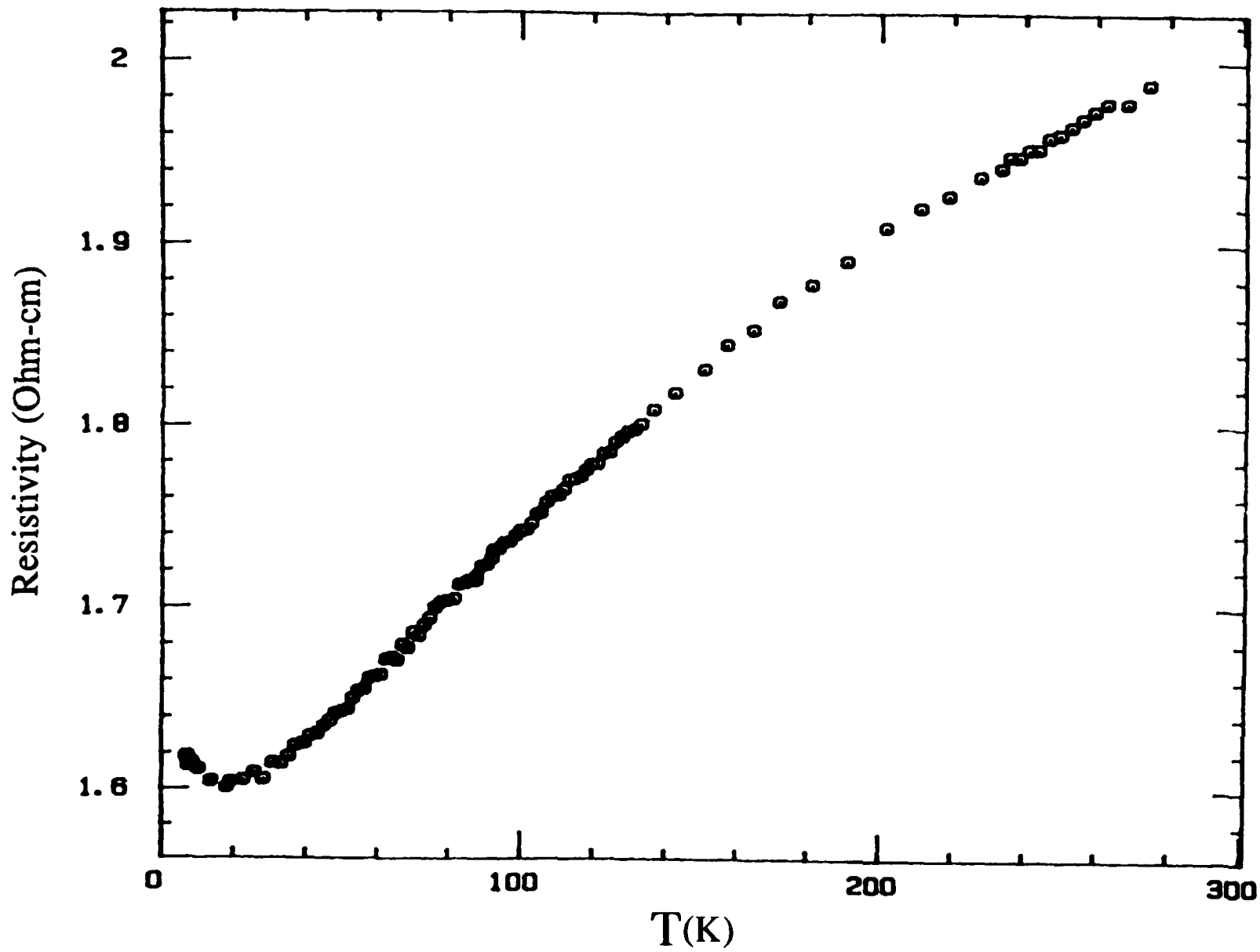

Ca$_3$MN. Chen et al Fig 5

TECHNICAL REPORT DISTRIBUTION LIST - GENERAL

Office of Naval Research (2)*
Chemistry Division, Code 1113
800 North Quincy Street
Arlington, Virginia 22217-5000

Dr. James S. Murday (1)
Chemistry Division, Code 6100
Naval Research Laboratory
Washington, D.C. 20375-5000

Dr. Robert Green, Director (1)
Chemistry Division, Code 385
Naval Weapons Center
China Lake, CA 93555-6001

Dr. Eugene C. Fischer (1)
Code 2840
David Taylor Research Center
Annapolis, MD 21402-5067

Dr. Elek Lindner (1)
Naval Ocean Systems Center
Code 52
San Diego, CA 92152-5000

Commanding Officer (1)
Naval Weapons Support Center
Dr. Bernard E. Douda
Crane, Indiana 47522-5050

Dr. Richard W. Drisko (1)
Naval Civil Engineering
Laboratory
Code L52
Port Hueneme, CA 93043

Dr. Harold H. Singerman (1)
David Taylor Research Center
Code 283
Annapolis, MD 21402-5067

Chief of Naval Research (1)
Special Assistant for Marine
Corps Matters
Code 00MC
800 North Quincy Street
Arlington, VA 22217-5000

Defense Technical Information
Center (2)
Building 5, Cameron Station
Alexandria, VA 22314

* Number of copies to forward

Enclosure (2)